$\gamma^* N \rightarrow N\pi$

S—wave multipole amplitudes and matrix elements

on Lattice

Yusheng Gao

School of Physics, Peking University

collaborate with ***Xu Feng, Zhaolong Zhang, Luchang Jin***
Ulf-G Meißner

Lattice 2024

29 July 2024

Background

- Nucleon has complicated QCD dynamical structure.
- Substituting electric current by weak current, this process is converted to neutrino-nucleon scattering process.
- Understanding pion photoproduction process from first principle is essential for us to understand QCD dynamics.
- LatticeQCD can achieve the energy regions that are difficult to be covered experimentally
- Information from both resonance and non-resonance channel is needed to improve the theorical precision

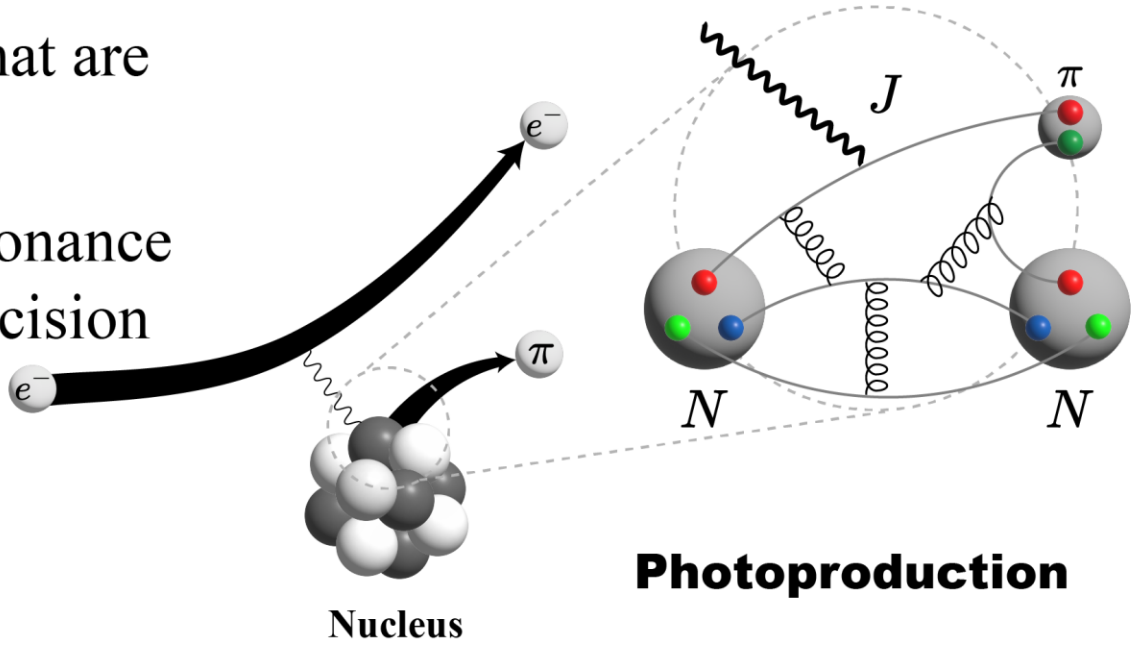

Experiement Situation

WILLIAM J. BRISCOE *et al.* PHYSICAL REVIEW C **108**, 065205 (2023)

TABLE I. Published data for $\gamma N \to \pi N$ reactions since 2012 as given in the SAID database [32]: first column is the reaction, second column is the observable, third column is the number of energy bins, fourth column is the number of data points.

Reaction	Observable	Nexp	Ndata	E_γ(min) (MeV)	E_γ(max) (MeV)	θ(min) (deg)	θ(max) (deg)	Laboratory/Collaboration	Ref.
$\gamma p \to \pi^0 p$	$d\sigma/d\Omega$	30	600	147	218	18	162	MAMI/A2	[39]
		269	7978	218	1573	15	165	MAMI/A2	[40]
		41	560	862	2475	15	165	CBELSA/CBELSA/TAPS	[41]
		80	2030	1275	5425	27	140	JLab/CLAS	[42]
		22	350	1325	2375	47	162	SPring-8/LEPS2&BGOegg	[43]
	Σ	26	220	147	206	25	155	MAMI/A2	[39]
		78	1403	319	649	31	158	MAMI/A2	[44]
		39	700	1102	1862	32	148	JLab/CLAS	[34]
		16	252	1325	2350	57	162	SPring-8/LEPS2&BGOegg	[43]
	$\mathbb{P}$	8	152	683	917	51	163	CBELSA/CBELSA/TAPS	[45]
		11	11	1845	5631	79	143	JLab/GEp-III & GEp2gamma	[46]
	$\mathbb{T}$	245	4343	151	419	5	175	MAMI/A2	[47]
		34	397	440	1430	30	162	MAMI/A2	[48]
		29	601	683	2805	29	163	CBELSA/CBELSA/TAPS	[45]
	$\mathbb{E}$	33	456	615	2250	22	158	CBELSA/CBELSA/TAPS	[49]
	$\mathbb{G}$	22	197	632	2187	37	144	JLab/CLAS	[50]
		19	318	633	1300	23	156	CBELSA/CBELSA/TAPS	[51]
	$\mathbb{F}$	34	397	440	1430	30	162	MAMI/A2	[48]
	$\mathbb{H}$	8	154	683	917	51	163	CBELSA/CBELSA/TAPS	[45]
	$\mathbb{C}_{x'}$	45	45	462	1337	75	140	MAMI/A2	[52]
		13	13	1845	5643	82	143	JLab/GEp-III & GEp2gamma	[46]
	$\mathbb{C}_{z'}$	13	13	1845	5643	80	143	JLab/GEp-III & GEp2gamma	[46]
$\gamma p \to \pi^+ n$	Σ	39	386	1102	1862	32	148	JLab/CLAS	[34]
	$\mathbb{E}$	35	900	363	2181	20	146	JLab/CLAS	[53]
	$\mathbb{G}$	22	216	632	2229	29	142	MAMI/A2	[50]
$\gamma n \to \pi^- p$	$\sigma_{t\alpha}$	6	6	150	162			MAX-lab/PIONS@MAX-lab	[54]
	$d\sigma/d\Omega$	14	104	301	455	58	133	MAMI/A2	[55]
		156	8428	445	2510	26	128	JLab/CLAS	[35]
		68	816	1050	3500	32	157	JLab/CLAS	[33]
	Σ	93	1293	947	2498	24	145	JLab/CLAS	[56]
	$\mathbb{E}$	21	266	727	2345	26	154	JLab/CLAS	[36]
$\gamma n \to \pi^0 n$	$d\sigma/d\Omega$	27	492	290	813	32	139	MAMI/A2	[37]
		49	931	446	1427	32	162	MAMI/A2	[57]
	Σ	12	189	390	610	49	148	MAMI/A2	[29]
	$\mathbb{E}$	17	151	446	1427	46	154	MAMI/A2	[58]

- Much data have been published by JLab/-CLAS, MAMI/A2, CBELSA/CBEL-SA/TAPS, SPring-8/LEPS2&BGOegg, JLab/GEp-III & GEp2gamma
- Partial Wave Amplitude can be extracted
- There are lots of methods to analyze experiments e.g. ANL-Osaka, SAID, MAID, the Bonn-Gatchina, Kent State, and JPAC groups and Julich-Bonn.

OnGoing Neutrino Experiment

Snow mass arXiv:2203.09030	Process	Neutrino Energy Range	Example Final State
Low Energy Nuclear Processes	Coherent Elastic Scattering	$\lesssim 50$ MeV	$\nu + A$
E_ν~1-100MeV	Inelastic Scattering	$\lesssim 100$ MeV	$e + {}^{A}(Z+1)^{*}(\rightarrow {}^{A}(Z+1) + n\gamma)$
	Quasi-Elastic Scattering	100 MeV--1 GeV	$l + p + X$
	Two-Nucleon Emission	1 GeV	$l + 2N + X$
Intermediate Energy Cross Sections	Resonance Production	1--3 GeV	$l + \Delta(\rightarrow N + \pi) + X$
E_ν~0.1-20GeV	Shallow Inelastic Scattering	3--5 GeV	$l + n\pi + X$
	Deep Inelastic Scattering	$\gtrsim 5$ GeV	$l + n\pi + X$

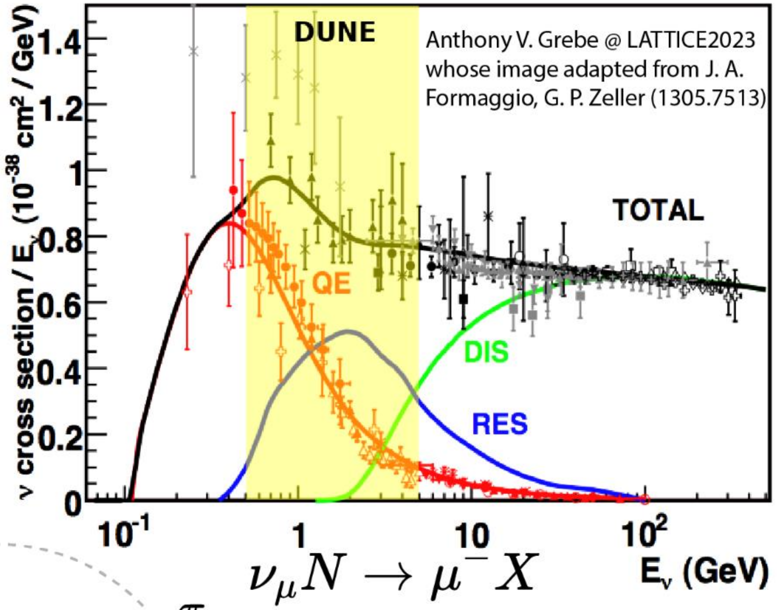

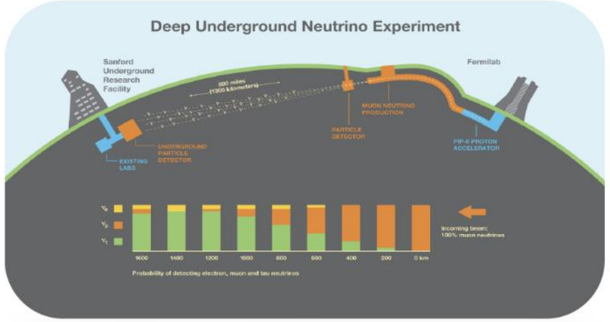

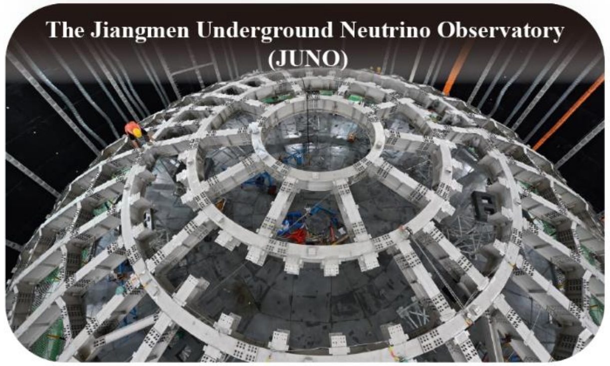

Lattice Calculable

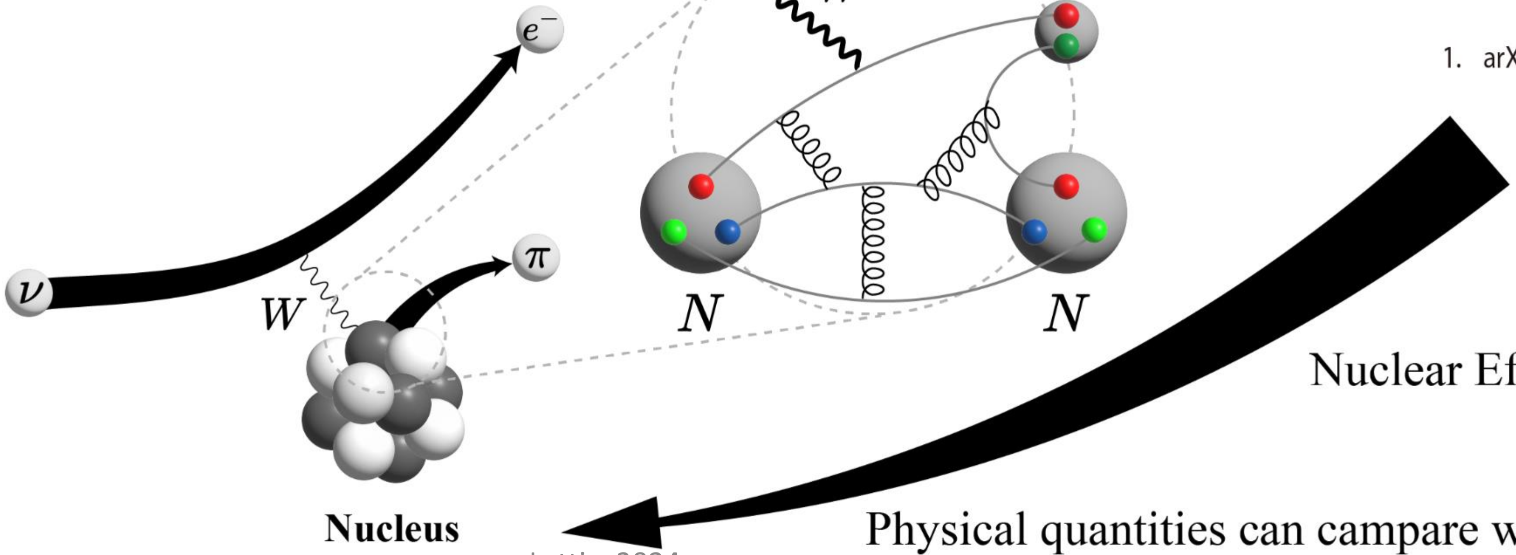

1. arXiv:2203.06853

Lattice QCD

Nuclear Effective theories

Physical quantities can campare with Experiment

Recent similar Lattice Attempts

- Main focus on the spectrum of baryon spectrum.
- C. Alexandrou studied the Nπ and Δ resonance state energy spectra and scattering parameters at the physical mass point(C. Alexandrou, et al. Phys. Rev. D (109) 2024 3 034509)
- Anthony V. Grebe, Michael Wagman attempt Nππ systems in Lattice2023
- Earlier calculations focused on S-wave elastic nucleon-pion scattering and P-wave Δ channel at unphysical mass ensemble

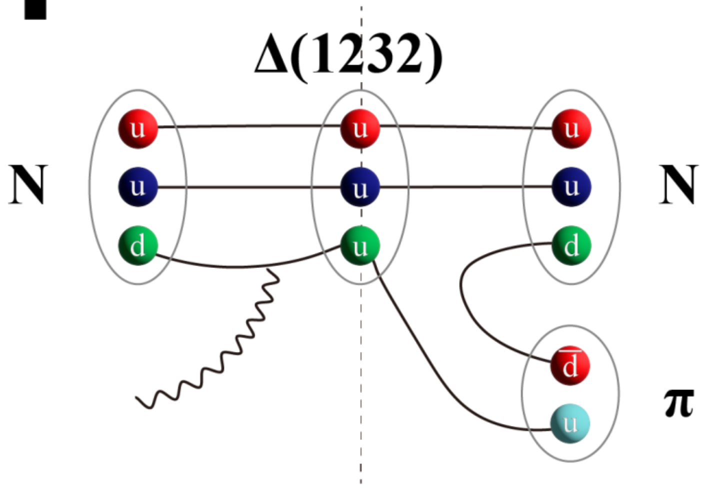

- John Bulava, Nuclear Physics B 987 (2023) 116105
- L. Barca, PHYSICAL REVIEW D 107, L051505 (2023)
- Giorgio Silvi, PHYSICAL REVIEW D 103, 094508 (2021)
- Christian Walther Andersen, PHYSICAL REVIEW D 97, 014506 (2018)
- C. B. Lang, PHYSICAL REVIEW D 95, 014510 (2017)

Lorentz Structure of Matrix element

Matrix elements can be decomposed into 8 form factors, using Lorentz invariance and the discrete symmetries C, P and T:

$$\langle N\pi|J^\mu|N\rangle = i\bar{u}_2\gamma_5\{\gamma^\mu \not{k} B_1 + 2P^\mu B_2 + 2q^\mu B_3 + 2k^\mu B_4 + \gamma^\mu B_5 + P^\mu \not{k} B_6 + k^\mu \not{k} B_7 + q^\mu \not{k} B_8\}u_1$$

By using Ward identity, only 6 form factors survive

$$\langle N\pi|J^\mu|N\rangle = i\bar{u}_2\gamma_5 \sum_{i=1}^{6} \mathcal{M}_i^\mu A_i(s,u) u_1$$

$$\mathcal{M}_1^\mu = \frac{1}{2}(\gamma^\mu \not{k} - \not{k}\gamma^\mu), \quad \mathcal{M}_2^\mu = P^\mu\left(2q\cdot k - k^2\right) - P\cdot k(2q^\mu - k^\mu),$$

$$\mathcal{M}_3^\mu = \gamma^\mu q\cdot k - \not{k} q^\mu, \quad \mathcal{M}_4^\mu = 2\gamma^\mu P\cdot k - 2\not{k}P^\mu - m\gamma^\mu\not{k} + m\not{k}\gamma^\mu,$$

$$\mathcal{M}_5^\mu = k^\mu q\cdot k - q^\mu k^2, \quad \mathcal{M}_6^\mu = k^\mu \not{k} - \gamma^\mu k^2$$

Low Energy Thereom

At threshold, the transition current matrix element be decomposed into corresponding multipoles, which are the function of two dimensionless parameter μ and ν.

V. Bernard, N. Kaiser, T. S. H. Lee and U.-G. Meißner Phys. Rep. 246 (1994) 6 315-363

$$\left\langle N_f \pi | \vec{J} | N_i \right\rangle = 4\pi i (1+\mu) \chi_f^{\dagger} \left\{ E_{0+}(\mu,\nu)\vec{\sigma} + [L_{0+}(\mu,\nu) - E_{0+}(\mu,\nu)] \hat{k} \sigma \cdot \hat{k} \right\} \chi_i$$

where $$\mu = \frac{m_\pi}{m_p}, \nu = \frac{k^2}{m_p^2}$$

E_0^+ and L_0^+ correspond to transverse and longitudinal contribution, respectively.

Lattice Setup

- The ensemble is generated by RBC and UKQCD Collaborations(T. Blum *et al.* (RBC, UKQCD), Phys. Rev. D **93**, 074505 (2016) 93)
- with Physical Pion Mass : 32Dfine
- Two correlation functions

$$C_{NJN\pi}(t_i, t, t_f, \vec{p}) = \langle O_{N\pi}(t_f) J^{\mu}(t, \vec{p}) \bar{O}_N(t_i, -\vec{p}) \rangle$$
$$C_{N\pi}(t_i, t_f,) = \langle O_{N\pi} \bar{O}_{N\pi} \rangle$$

- For accelerating contraction calculation and getting better sign:
  - Using the random sparsening-field technique
  - Smearing sparsening-field.

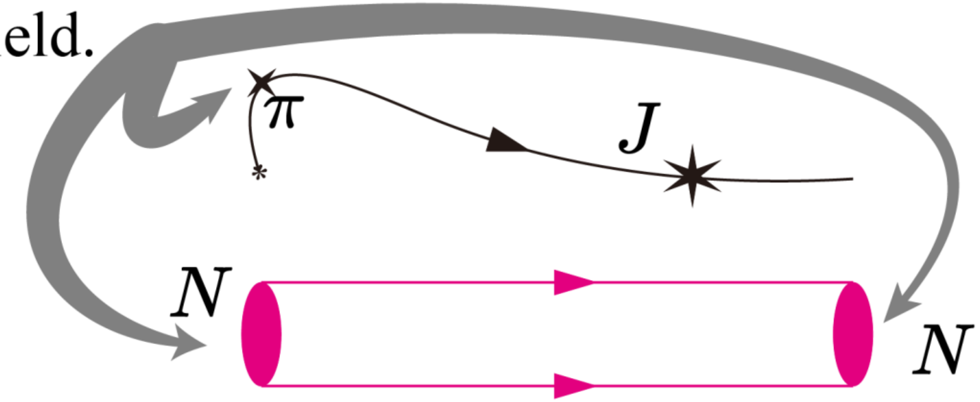

Y. Li, S.-C. Xia, X. Feng, L.-C. Jin, and C. Liu, Phys. Rev. D 103, 014514 (2021), arXiv:2009.01029 [hep-lat].

W. Detmold, D. J. Murphy, A. V. Pochinsky, M. J. Savage, P. E. Shanahan, and M. L. Wagman, Phys. Rev. D

Contration detail for $C_{NJN\pi}$ $C_{N\pi N\pi}$

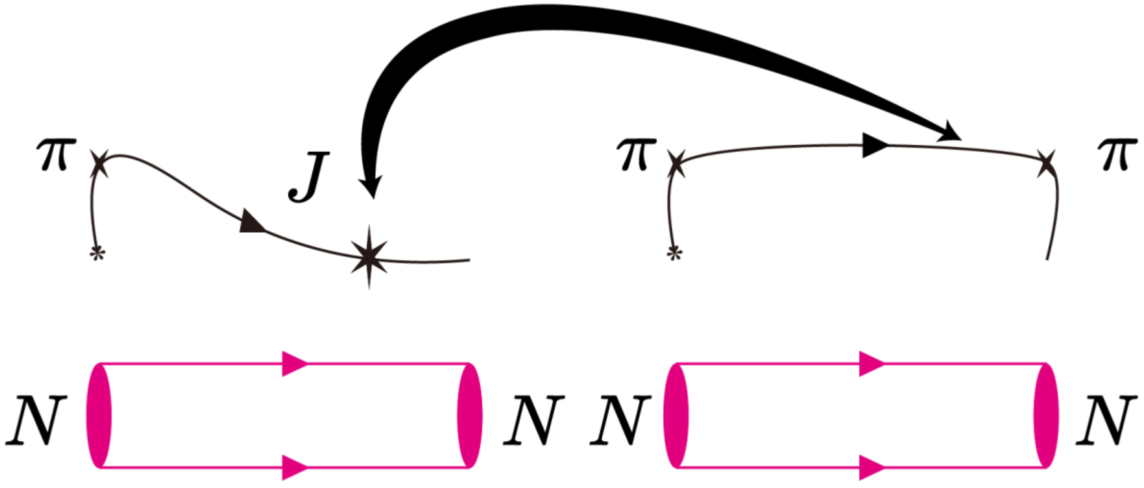

22 topologies digrams
should be considered.

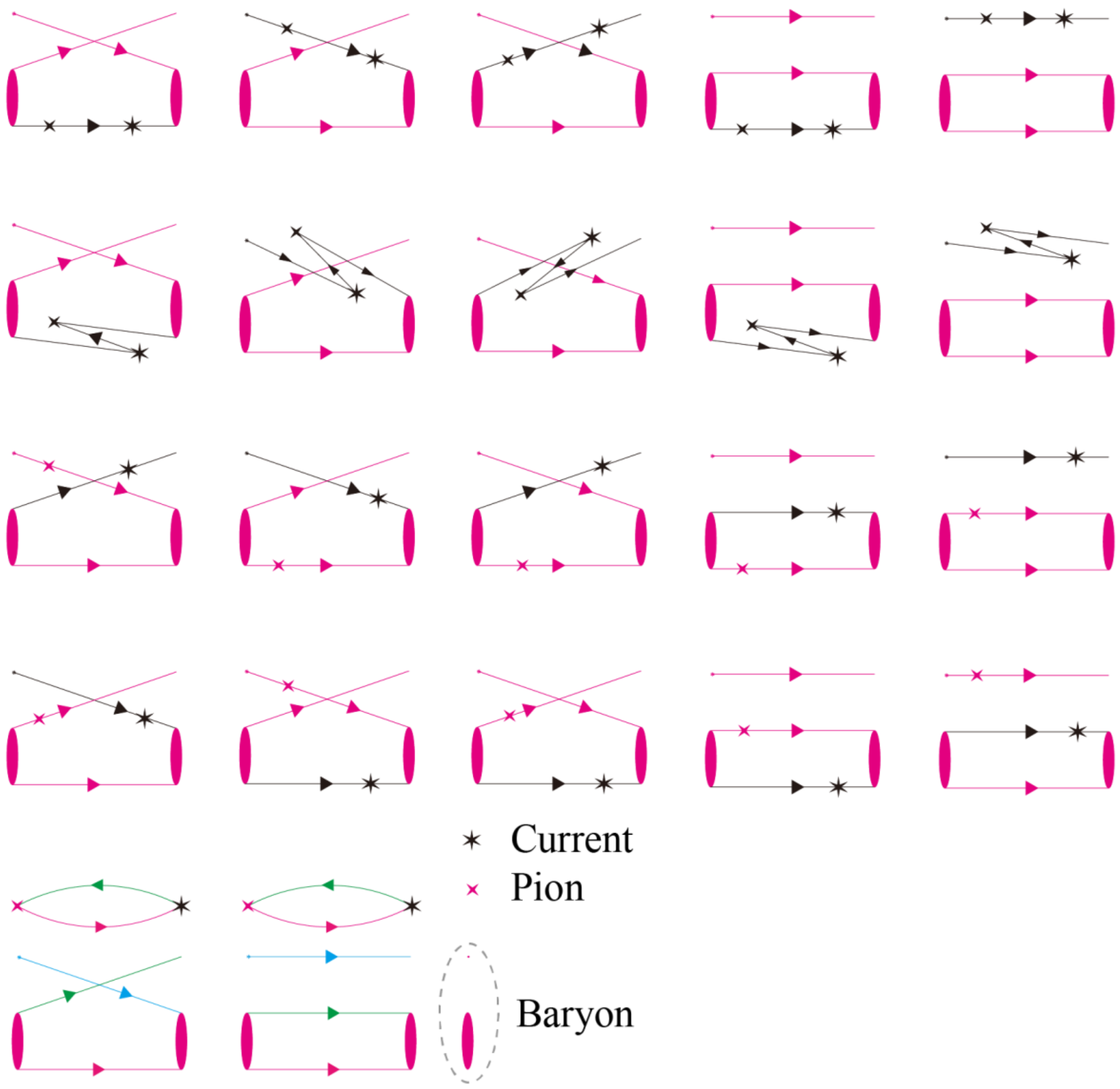

Extract Matrix element

Normalization for $_I\left\langle N\pi \middle| J_i^{I'} \middle| N \right\rangle$

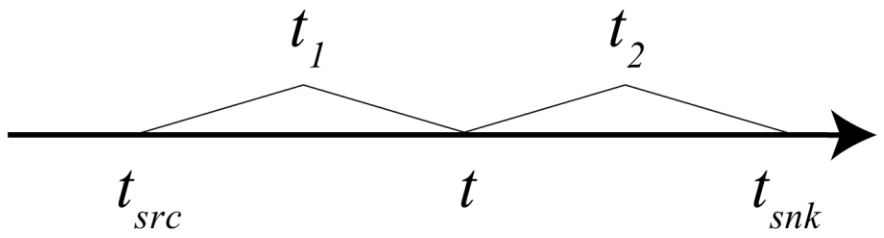

$$R = \frac{C_{NJN\pi}(t_1, t_2)}{C_{N\pi}(t_1 + t_2)} \times \sqrt{\frac{C_N(t_1) C_{N\pi}(t_2) C_{N\pi}(t_1 + t_2)}{C_{N\pi}(t_1) C_N(t_2) C_N(t_1 + t_2)}}$$

Summation insertion (Maiani L. NPB, 293, 420(1987))

$$S(T_s) = \sum_{t_1 + t_2 = T_s} R(t_1, t_2)$$

$$\xrightarrow{T_s \to \infty} c_0 + \frac{1}{\sqrt{2M}} {}_I\left\langle N\pi \middle| J_i^{I'} \middle| N \right\rangle \cdot T_S$$

Linear fit

Extract Matrix element of $\vec{p} = 0$

Xuanhe Wang,
Zhaolong Zhang
2310.01168

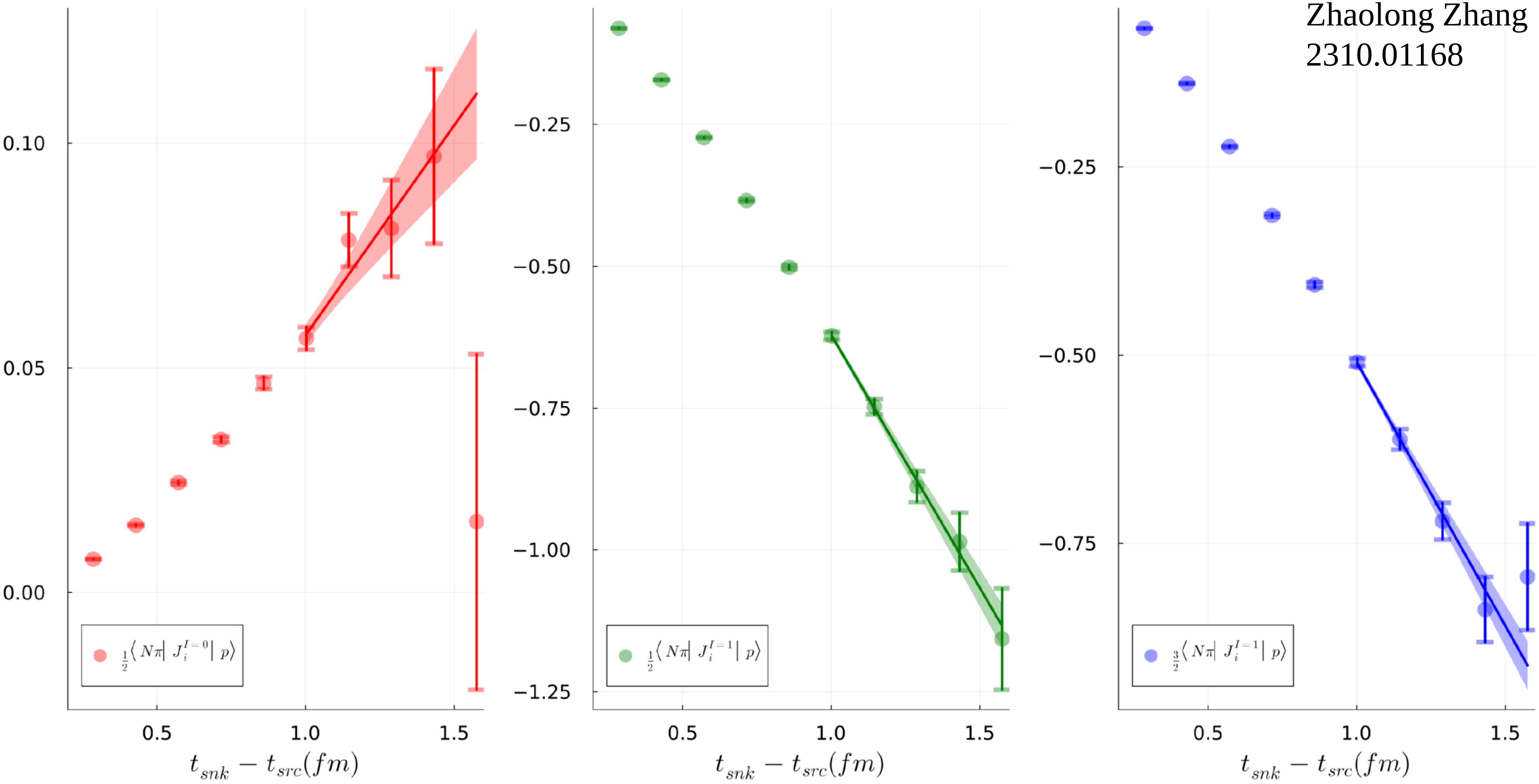

Extract Matrix element

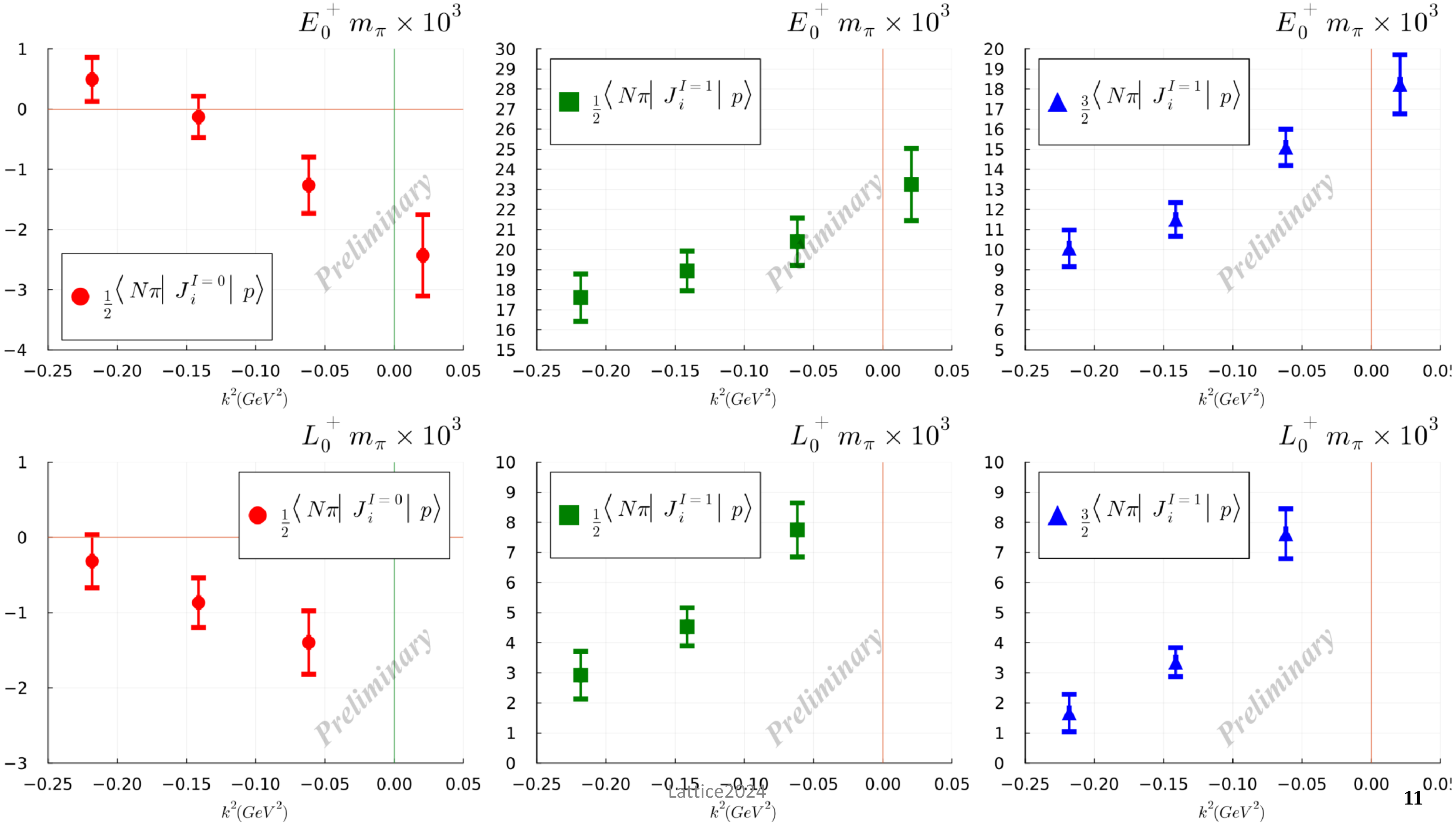

LL factor and Nπ spectrum

Although Energy shift and scattering length can be extracted only by Nπ interpolators which N and π are static, GEVP can make a change.

$$R = \frac{C_2^{N\pi}(t)}{C_2^N(t)C_2^\pi(t)} \approx 1 - \Delta E t$$

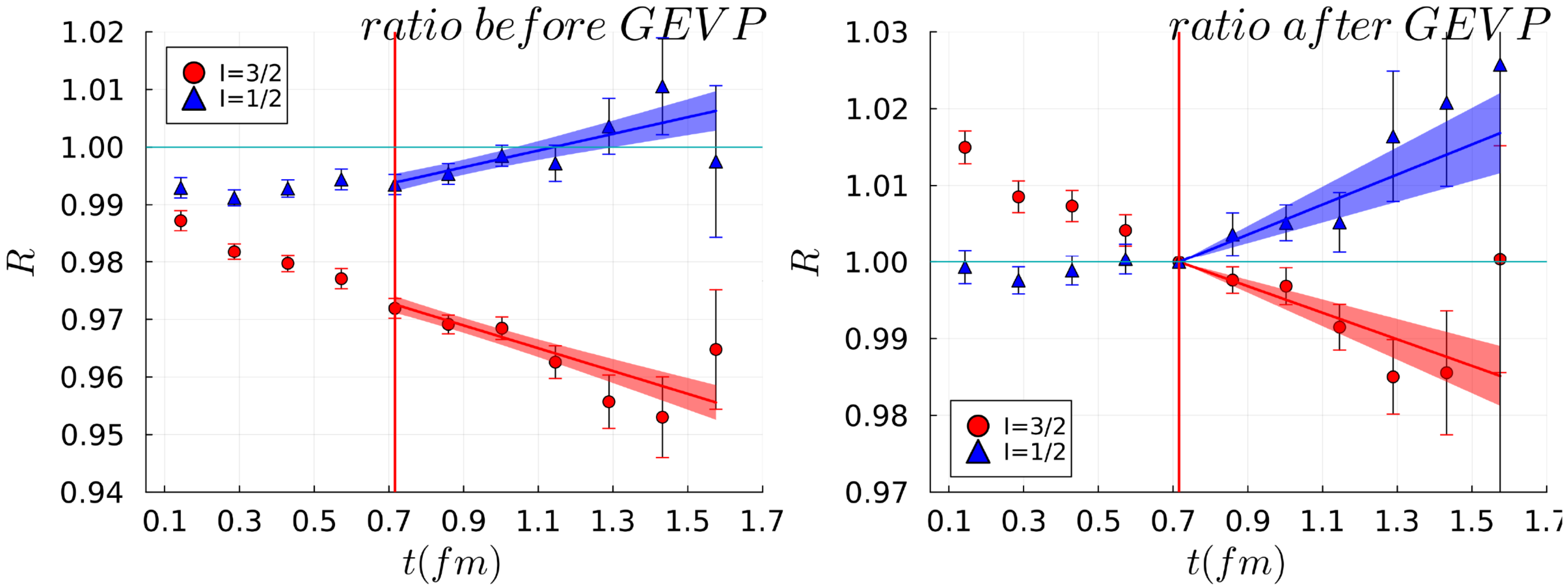

LL factor and Nπ spectrum

The result before GEVP is consistent with

$$M_\pi a_0^{\frac{1}{2}} = 0.127(24) \quad M_\pi a_0^{\frac{1}{2}} = -0.127(14)$$

The result after GEVP is consistent with

$$M_\pi a_0^{\frac{1}{2}} = 0.152(28) \quad M_\pi a_0^{\frac{1}{2}} = -0.107(17)$$

the data-driven analysis (by Martin Hoferichter and et al. Phys. Lett. B 843, 138001 (2023))

$$M_\pi a_0^{\frac{1}{2}} = 0.170(2) \quad M_\pi a_0^{\frac{1}{2}} = -0.087(2)$$

Extract Matrix element

Thanks to T. S. H. Lee suggestion. The PWA fit result by ANL-Osaka group from experiment data is shown. https://www.phy.anl.gov/theory/research/anl-osaka-pwa/

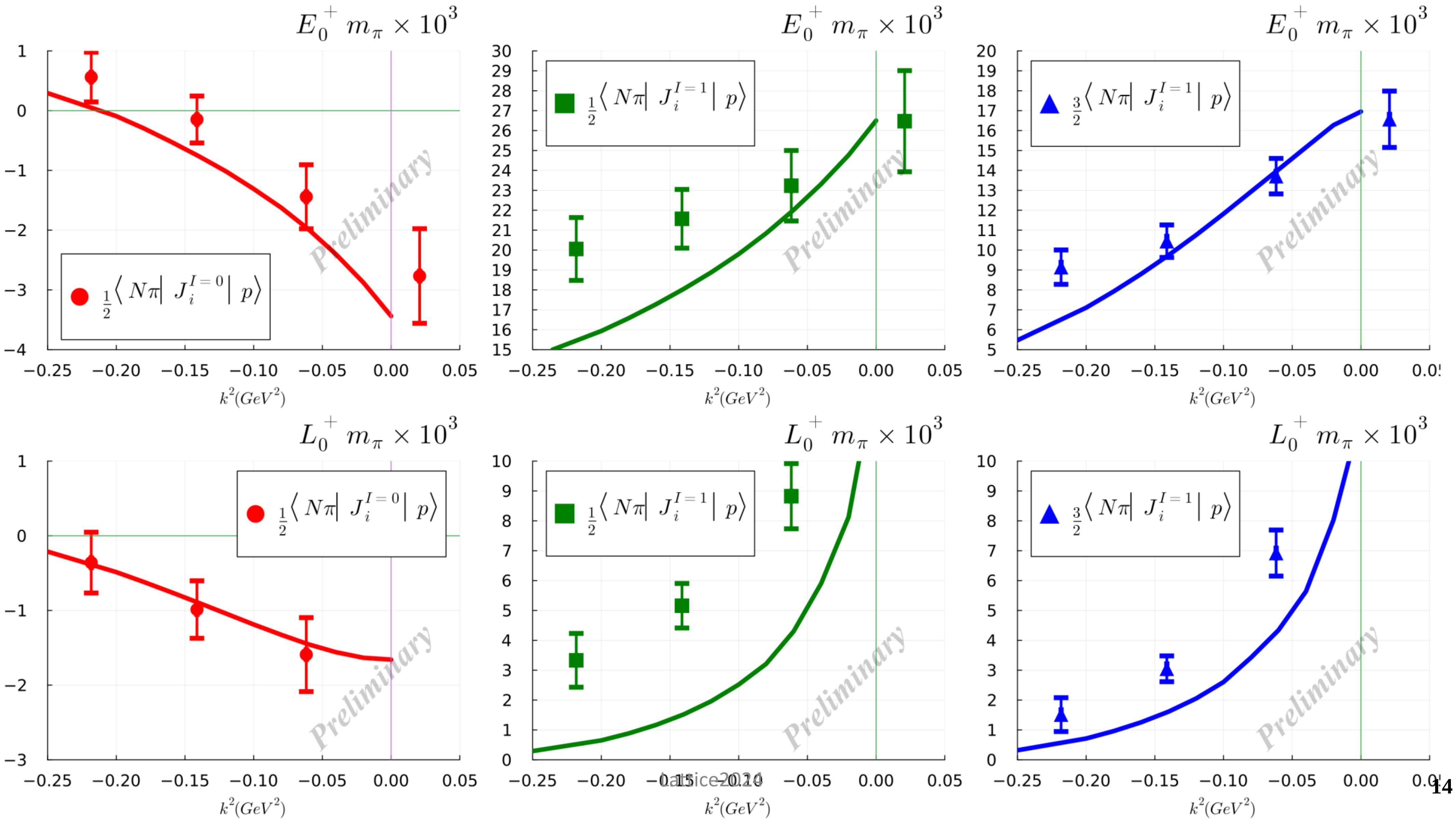

Conculsion

- We calculate S-wave mutipole amplitude E_0^+ and L_0^+
- This methodology can be easily expanded to weak pion production process
- Other channels like Δ-resonance ηN, πΣ are also worth to explore.
- Our ultimate goal is to improve the computational accuracy of each reaction channel to illuminate the path to new physics.

Thanks for your attention!!!

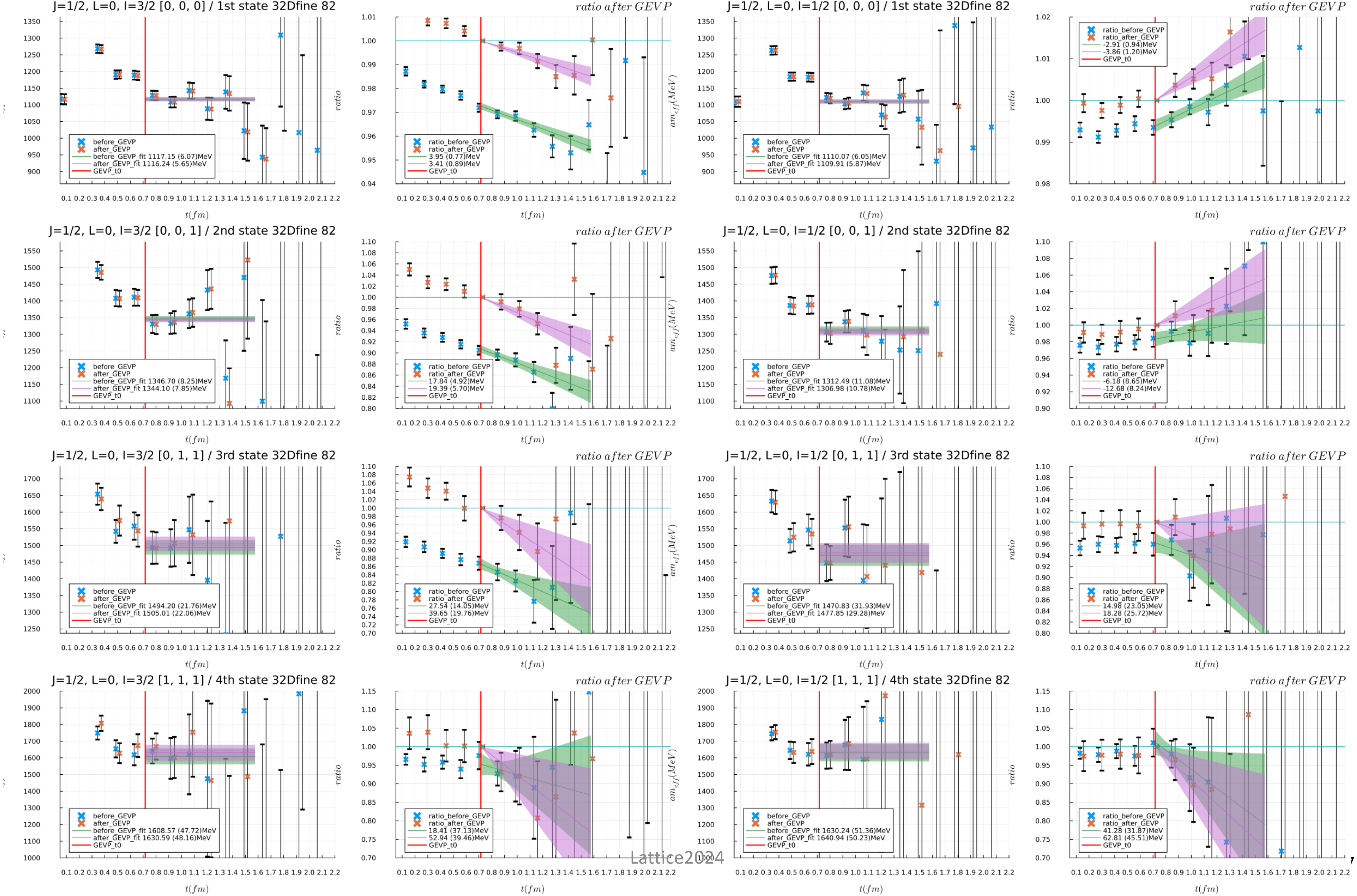

J=1/2, L=0, I=3/2 [0, 0, 0] / 1st state 32Dfine 82
before_GEVP
after_GEVP
before_GEVP_fit 1117.15 (6.07)MeV
after_GEVP_fit 1116.24 (5.65)MeV
GEVP_t0
ratio after GEVP
ratio_before_GEVP
ratio_after_GEVP
3.95 (0.77)MeV
3.41 (0.89)MeV
GEVP_t0
J=1/2, L=0, I=1/2 [0, 0, 0] / 1st state 32Dfine 82
before_GEVP
after_GEVP
before_GEVP_fit 1110.07 (6.05)MeV
after_GEVP_fit 1109.91 (5.87)MeV
GEVP_t0
ratio after GEVP
ratio_before_GEVP
ratio_after_GEVP
-2.91 (0.94)MeV
-3.86 (1.20)MeV
GEVP_t0
J=1/2, L=0, I=3/2 [0, 0, 1] / 2nd state 32Dfine 82
before_GEVP
after_GEVP
before_GEVP_fit 1346.70 (8.25)MeV
after_GEVP_fit 1344.10 (7.85)MeV
GEVP_t0
ratio after GEVP
ratio_before_GEVP
ratio_after_GEVP
17.84 (4.92)MeV
19.39 (5.70)MeV
GEVP_t0
J=1/2, L=0, I=1/2 [0, 0, 1] / 2nd state 32Dfine 82
before_GEVP
after_GEVP
before_GEVP_fit 1312.49 (11.08)MeV
after_GEVP_fit 1306.98 (10.78)MeV
GEVP_t0
ratio after GEVP
ratio_before_GEVP
ratio_after_GEVP
-6.18 (8.65)MeV
-12.68 (8.24)MeV
GEVP_t0
J=1/2, L=0, I=3/2 [0, 1, 1] / 3rd state 32Dfine 82
before_GEVP
after_GEVP
before_GEVP_fit 1494.20 (21.76)MeV
after_GEVP_fit 1505.01 (22.06)MeV
GEVP_t0
ratio after GEVP
ratio_before_GEVP
ratio_after_GEVP
27.54 (14.05)MeV
39.65 (19.76)MeV
GEVP_t0
J=1/2, L=0, I=1/2 [0, 1, 1] / 3rd state 32Dfine 82
before_GEVP
after_GEVP
before_GEVP_fit 1470.83 (31.93)MeV
after_GEVP_fit 1477.85 (29.28)MeV
GEVP_t0
ratio after GEVP
ratio_before_GEVP
ratio_after_GEVP
14.98 (23.05)MeV
18.28 (25.72)MeV
GEVP_t0
J=1/2, L=0, I=3/2 [1, 1, 1] / 4th state 32Dfine 82
before_GEVP
after_GEVP
before_GEVP_fit 1608.57 (47.72)MeV
after_GEVP_fit 1630.59 (48.16)MeV
GEVP_t0
ratio after GEVP
ratio_before_GEVP
ratio_after_GEVP
18.41 (37.13)MeV
52.94 (39.46)MeV
GEVP_t0
J=1/2, L=0, I=1/2 [1, 1, 1] / 4th state 32Dfine 82
before_GEVP
after_GEVP
before_GEVP_fit 1630.24 (51.36)MeV
after_GEVP_fit 1640.94 (50.23)MeV
GEVP_t0
ratio after GEVP
ratio_before_GEVP
ratio_after_GEVP
41.28 (31.87)MeV
62.81 (45.51)MeV
GEVP_t0
$t(fm)$
$am_{eff}(MeV)$
ratio

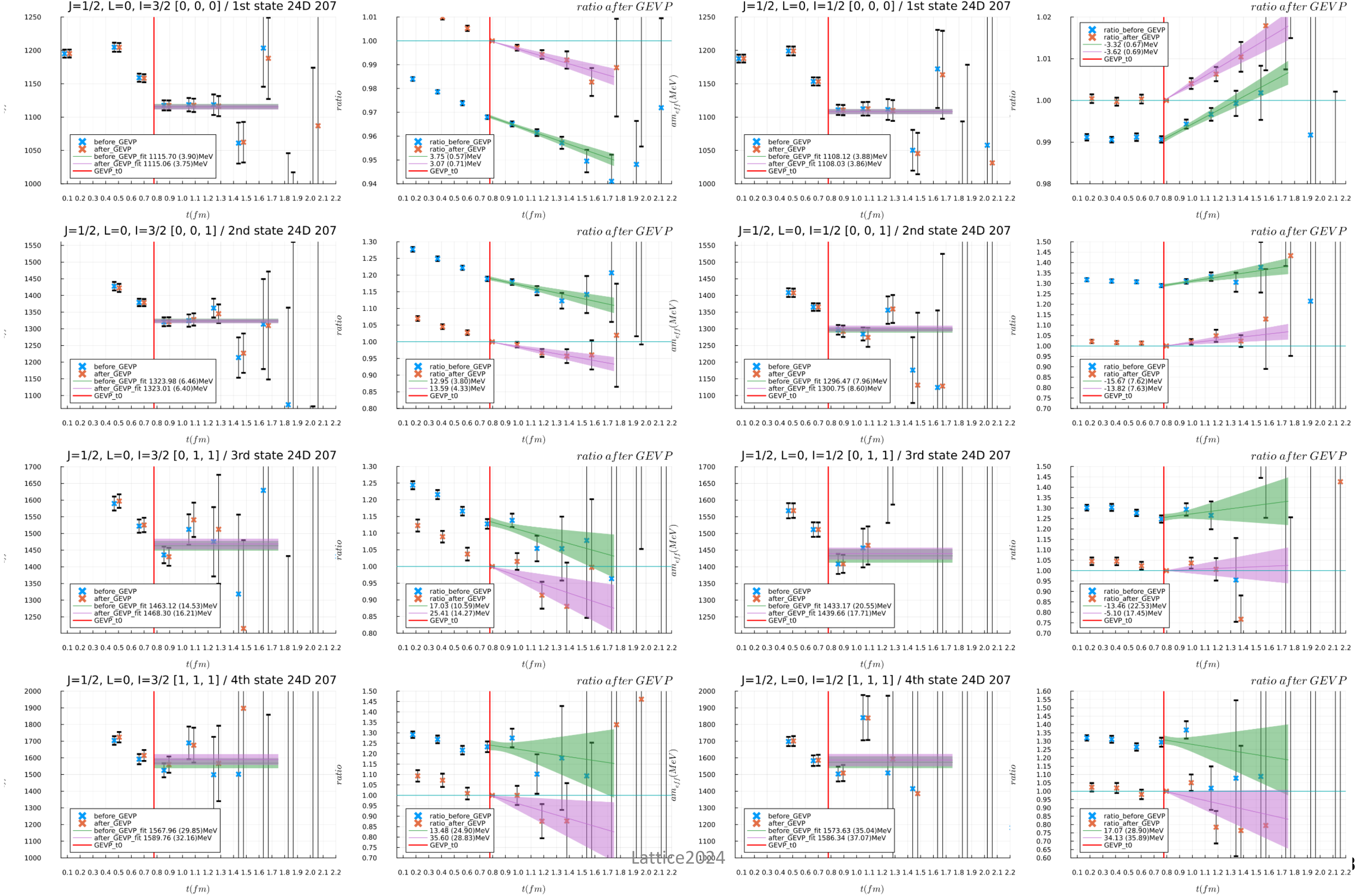

J=1/2, L=0, I=3/2 [0, 0, 0] / 1st state 24D 207
before_GEVP
after_GEVP
before_GEVP_fit 1115.70 (3.90)MeV
after_GEVP_fit 1115.06 (3.75)MeV
GEVP_t0
ratio after GEVP
ratio_before_GEVP
ratio_after_GEVP
3.75 (0.57)MeV
3.07 (0.71)MeV
GEVP_t0
J=1/2, L=0, I=1/2 [0, 0, 0] / 1st state 24D 207
before_GEVP
after_GEVP
before_GEVP_fit 1108.12 (3.88)MeV
after_GEVP_fit 1108.03 (3.86)MeV
GEVP_t0
ratio after GEVP
ratio_before_GEVP
ratio_after_GEVP
-3.32 (0.67)MeV
-3.62 (0.69)MeV
GEVP_t0
J=1/2, L=0, I=3/2 [0, 0, 1] / 2nd state 24D 207
before_GEVP
after_GEVP
before_GEVP_fit 1323.98 (6.46)MeV
after_GEVP_fit 1323.01 (6.40)MeV
GEVP_t0
ratio after GEVP
ratio_before_GEVP
ratio_after_GEVP
12.95 (3.80)MeV
13.59 (4.33)MeV
GEVP_t0
J=1/2, L=0, I=1/2 [0, 0, 1] / 2nd state 24D 207
before_GEVP
after_GEVP
before_GEVP_fit 1296.47 (7.96)MeV
after_GEVP_fit 1300.75 (8.60)MeV
GEVP_t0
ratio after GEVP
ratio_before_GEVP
ratio_after_GEVP
-15.67 (7.62)MeV
-13.82 (7.63)MeV
GEVP_t0
J=1/2, L=0, I=3/2 [0, 1, 1] / 3rd state 24D 207
before_GEVP
after_GEVP
before_GEVP_fit 1463.12 (14.53)MeV
after_GEVP_fit 1468.30 (16.21)MeV
GEVP_t0
ratio after GEVP
ratio_before_GEVP
ratio_after_GEVP
17.03 (10.59)MeV
25.41 (14.27)MeV
GEVP_t0
J=1/2, L=0, I=1/2 [0, 1, 1] / 3rd state 24D 207
before_GEVP
after_GEVP
before_GEVP_fit 1433.17 (20.55)MeV
after_GEVP_fit 1439.66 (17.71)MeV
GEVP_t0
ratio after GEVP
ratio_before_GEVP
ratio_after_GEVP
-13.46 (22.53)MeV
-5.10 (17.45)MeV
GEVP_t0
J=1/2, L=0, I=3/2 [1, 1, 1] / 4th state 24D 207
before_GEVP
after_GEVP
before_GEVP_fit 1567.96 (29.85)MeV
after_GEVP_fit 1589.76 (32.16)MeV
GEVP_t0
ratio after GEVP
ratio_before_GEVP
ratio_after_GEVP
13.48 (24.90)MeV
35.60 (28.83)MeV
GEVP_t0
J=1/2, L=0, I=1/2 [1, 1, 1] / 4th state 24D 207
before_GEVP
after_GEVP
before_GEVP_fit 1573.63 (35.04)MeV
after_GEVP_fit 1586.34 (37.07)MeV
GEVP_t0
ratio after GEVP
ratio_before_GEVP
ratio_after_GEVP
17.07 (28.90)MeV
34.13 (35.89)MeV
GEVP_t0
t(fm)
ratio
am_eff(MeV)
Lattice2024